International Journal of Nanomedicine

Dovepress
Taylor & Francis Group

Open Access Full Text Article

ORIGINAL RESEARCH

Zeolitic Imidazolate Framework-90 Treats Fungal Keratitis by Promoting Macrophage Apoptosis and Targeting Increased Mitochondrial Reactive Oxygen Species in Aspergillus Fumigatus

Xueyun Fu[1], Lina Zhang[1], Jing Lin[1], Qian Wang[1], Ziyi Wang[1], Menghui Chi[1], Daohao Li[2], Guiqiu Zhao[1], Cui Li[1]

[1]Department of Ophthalmology, The Affiliated Hospital of Qingdao University, Qingdao, People's Republic of China; [2]State Key Laboratory of Bio-fibers and Eco-Textiles, Institute of Marine Biobased Materials, College of Materials Science and Engineering, Qingdao University, Qingdao, People's Republic of China

Correspondence: Guiqiu Zhao; Cui Li, Department of Ophthalmology, Affiliated Hospital of Qingdao University, 16 Jiangsu Road, Qingdao, Shandong, 266003, People's Republic of China, Email zhaoguiqiu_good@126.com; yankelicui@126.com

Background: Fungal keratitis is a severe vision-threatening corneal infection with a prognosis influenced by fungal virulence and the host's immune defense mechanisms. However, there is still a lack of effective drugs that attenuate fungal virulence while relieving the inflammatory response caused by fungal keratitis.

Purpose: Finding an effective treatment to solve these problems is particularly important.

Methods: We synthesized Zeolitic imidazolate framework-90 (ZIF-90) by water-based synthesis method and characterized it. In vitro experiments included mycelium electron microscopy, Cell Counting Kit-8 (CCK-8), and Enzyme-linked immunosorbent assay (ELISA). These trials verified the disruptive effects of ZIF-90 on morphology, cell membrane, cell wall, and biofilm formation of Aspergillus fumigatus (*A. fumigatus*). These experiments also demonstrated the impact of ZIF-90 on the proinflammatory cytokines tumor necrosis factor-α (TNF-α) and interleukin-6 (IL-6). Moreover, the effect of ZIF-90 on mitochondrial reactive oxygen species (mtROS) of cells and fungi was verified by MitoSOX Red Mitochondrial Superoxide Indicator (MitoSOX). In vivo, corneal toxicity test, establishment and treatment of mycotic keratitis mouse model, and immunofluorescence staining were used to evaluate the efficacy of ZIF-90 in the procedure of fungal keratitis. In addition, to investigate whether the metal-ligand zinc and the organic ligand imidazole acted as essential factors in ZIF-90, we investigated the in vitro antimicrobial and anti-inflammatory effects of ZIF-8, ZIF-67 and Metal-Organic Frameworks-74 (Zn) (MOF-74 (Zn)) by Minimum Inhibitory Concentration (MIC) and ELISA experiments.

Results: ZIF-90 has therapeutic effects on fungal keratitis, which could break the protective organelles of *A. fumigatus*, such as the cell wall. In addition, ZIF-90 can also be targeted to increase the amount of mtROS in fungi and promote apoptosis of macrophages. The results demonstrated that both zinc ions and imidazole possessed antimicrobial and anti-inflammatory effects. In addition, ZIF-90 exhibited better antifungal properties than ZIF-8, ZIF-67, and MOF-74 (Zn).

Keywords: zeolite imidazolate framework, nanomedicine, fungal infection, keratitis

Introduction

Fungal keratitis is a serious blinding eye disease that can lead to permanent vision loss.[1,2] Aspergillus is one of the main causative agents of fungal keratitis.[3] Fungal keratitis can occur for a variety of reasons, such as trauma, wearing corneal contact lenses, and overusing glucocorticoids. It is estimated that more than one million patients worldwide suffer from fungal keratitis each year, and about three-quarters of them are blind due to the disease.[2,4] Fungal keratitis has become a major public health problem in many countries, especially in developing countries. How to effectively and economically treat fungal keratitis remains a challenge.

Received: 13 January 2025
Accepted: 7 April 2025
Published: 12 April 2025

Reducing the virulence of the fungus and controlling the defenses of the host are key to the treatment of fungal keratitis, and this critical issue determines the prognosis of fungal keratitis. Host immune cells can counteract fungal infections, thereby limiting tissue damage caused by such infections. Bauer et al proved that subconjunctival macrophages are the first line of defense cells in the cornea, which promotes the secretion of inflammatory cytokines and recruits a variety of immune cells to help the host fight fungal infection.[5–7] Nevertheless, the overactivation of macrophages in the cornea leads to an excessive immune response. The excessive immune response brings about an uncontrollable inflammatory response that destroys the corneal stroma.[4,8,9] Thus, controlling the inflammatory response is particularly important in the treatment of fungal keratitis. Unfortunately, current therapeutic agents are unable to control the excessive inflammatory response, which poses a potential problem in the treatment of fungal keratitis. Moreover, these drugs have poor permeability and definite corneal toxicity. In this context, regulating mtROS levels has emerged as a therapeutic strategy.[10] Overproduction of mtROS in fungal cells can lead to metabolic disorders and promote their apoptosis, while the reduction of mtROS in host cells can decrease tissue oxidative damage and excessive inflammation.[10,11]

ZIF-90, as a kind of MOF material, has the advantages of excellent biocompatibility and low cytotoxicity.[12,13] In recent years, nano-delivery systems have been widely used in treating eye diseases due to their low toxicity and efficient delivery. ZIF-90, as a member of the nanocarrier, has a wide range of applications in targeted drug delivery, such as the delivery of metronidazole as a drug delivery agent for the treatment of sepsis.[14] These broad applications highlight the versatility and potential of ZIF-90 as a versatile material.[15–17] However, the immunogenicity and efficacy of ZIF-90 in the treatment of fungal keratitis remain unclear. ZIF-90 is composed of metal ions zinc and imidazole ligands. Zinc ion has been proven to have anti-inflammatory and antibacterial effects.[18–20] Azole drugs are a class of classical antifungal drugs widely used in clinical settings,[21,22] so this paper predicts that ZIF-90 may have therapeutic effects on fungal keratitis.

In this study, ZIF-90 was synthesized and characterized by the water-based synthesis method. Then, the anti-inflammatory and antifungal effects of ZIF-90 were studied using the spore adhesion test, ELISA, and other tests. We found that in vitro, ZIF-90 can inhibit the growth of *A. fumigatus* by destroying the cell wall cell membrane, reducing spore adhesion to Human corneal epithelial cells (HCECs), and controlling inflammatory responses by promoting macrophage apoptosis. In vivo, ZIF-90 can treat fungal keratitis by reducing the infiltration of inflammatory cells in the mouse cornea and the number of inflammatory factors. Finally, the antibacterial and anti-inflammatory effects of ZIF-8, ZIF-67, and MOF-74 (Zn) were verified in vitro, proving that both zinc ions and imidazole groups contained in ZIF-90 can inhibit the growth of *A. fumigatus* and have anti-inflammatory effects (Scheme 1). The presence of aldehyde groups on the imidazole group can improve the biocompatibility of ZIF-90.

Materials and Methods

Synthesis and Characterization of ZIF-90

A zinc nitrate aqueous solution was prepared as solution A, while imidazole-2-carboxaldehyde (ICA) and polyvinylpyrrolidone (PVP) were dissolved to form solution B. In the water/ethanol/PVP system, zinc nitrate was dissolved in an ethanol medium to form solution A. The amount of PVP and Zn^{2+} to ICA ratio was meticulously controlled. Solutions A and B were mixed at room temperature for 30 min. ZIF-90 was collected by centrifugation and thoroughly washed with methanol. The powder was vacuum-dried at 50 °C.[23] The shape and appearance of the samples were examined using a scanning electron microscope (SEM; JSM-7001F; JEOL, Tokyo, Japan), and the particle size of the samples was analyzed using Image J software. X-ray diffraction (XRD) analysis was conducted by using a Rigaku diffractometer (Japan) and employing x-ray radiation across a 5°-40° range, with a scanning rate set at 5° min^{-1}. X-ray photoelectron spectroscopy (XPS) was carried out using a VG Scientific ESCALab220i-XL spectrometer equipped with a monochromatic Al Kα X-ray source. Fourier Transform Infrared Spectrometer (FT-IR; Themo, USA) was used to measure the samples in the wavelength range of 1500 to 2500 cm^{-1}.

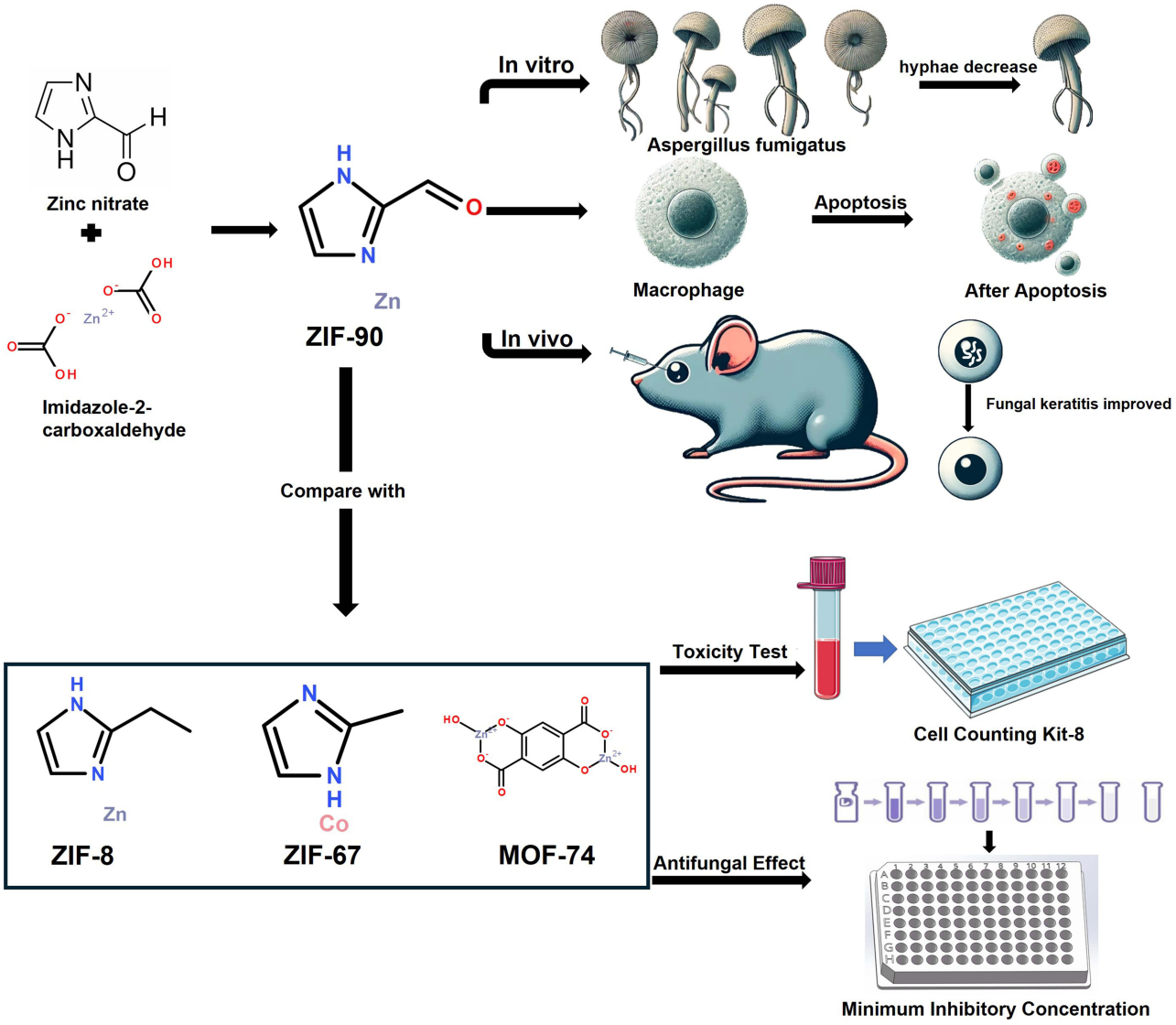

Scheme 1 The therapeutic effect of ZIF-90 on fungal keratitis and the comparison of anti-fungal and biocompatibility between ZIF-90 and other MOF materials.

Acquisition of A. Fumigatus Hyphae and Spores

A. fumigatus spores (Strain 3.0772, China General Microbiological Culture Collection Center) were placed in an aseptic Salter medium and cultured in a shaking table for 5–7 days (300 rpm, 37 °C). When the spores grew into hyphae and formed into balls, they were ground with a sterile grinding rod. After the hyphae were ground evenly, they were washed with Phosphate buffer saline (PBS; Solarbio). Then, the hyphae were soaked with 75% ethanol and placed in a refrigerator at 4 °C overnight for inactivation. Upon inactivation, the hyphae were washed with PBS and diluted with a high-sugar culture solution to a concentration of 1×10^8. The spores were cultured on sabouraud agar medium (SDA) (Hopebio, China) and washed with PBS. The spore suspension was diluted to a suitable concentration during usage.

HCECs Fungal Spore Adhesion Assay

HCECs were inoculated and cultured in a cell incubator following standard protocols.[24] The research involving HCECs received approval from the Ethics Review Committee of the Affiliated Hospital of Qingdao University, Qingdao, Shandong, China (Approval No. QYFYWZLL 29257). ZIF-90 (64 μg/mL) and spore suspension (1×10^7 CFU/mL)

https://doi.org/10.2147/IJN.S517169

were added when the cells grew into 30%-50% of the plate pore area. HCECs and spores were cultured for 3 h, and the culture medium was sucked out. Then, HCECs and spores were washed 3 times with sterile PBS and then fixed with methanol, next the methanol was sucked out and dried, and HCECs were stained by Hematoxylin-eosin (HE) staining and observed spore adhesion under a microscope (Axiovert; Zeiss, Jena, Germany, 400×).

Cell Viability Test

The Cell Counting Kit 8 (CCK-8) kit was used to detect the cytotoxicity of ZIF-8, ZIF-67, MOF-74 (Zn), and ZIF-90 against HCECs and RAW 264.7 cells. RAW 264.7 cells (Obtained from the Academy of Sciences in Shanghai) were inoculated onto 96-well plates. When the cells grew into 80% of the pore plate area, different concentrations (2, 4, 8, 16, 32, 64, 128 μg/mL) of ZIF-8, ZIF-67, MOF-74 (Zn) and ZIF-90 were added. The four MOF materials were added to cck-8 (HY-K0301) post 24 h of co-culture with cells, and the absorbance at 450 nm was measured after 1 h of culture.

MIC Experiment

A spore suspension of 3×10^5 CFU/mL was inoculated into a 96-well plate, followed by the addition of ZIF-8, ZIF-6, and ZIF-90 to achieve final concentrations of 2, 4, 8, 16, 32, 64, and 128 μg/mL, respectively. The 96-well plate was then incubated in a constant temperature incubator (37 °C, 5% CO_2) for 24 h to allow for co-cultivation of the compounds with the spores. The absorbance at 540 nm was measured as soon as the incubation period.

Biofilm Inhibition Experiment

The spore suspension of 3×10^5 CFU/mL and ZIF-90 of different concentrations (4, 8, 16, 32, 64, 128 μg/mL) were added to the 24-well plate. The spore and ZIF-90 were cultured in a constant temperature incubator (37 °C, 5% CO_2) for 24 h until thin hyphae grew. Then, the surface hyphae were removed with an insulin needle, and the sand culture medium was extracted. The biofilm in the bottom of the 24-well plate was washed with PBS 3 times and dried at room temperature. Once drying, the 99% methanol was added to the 24-well plate to fix the biofilm for 20 min. After removing the methanol, the biofilm was rinsed with sterile deionized water and dried at room temperature. Crystal violet stain was added to the plate and soaked at room temperature. After 15 min, the dye solution was removed, and the unbound crystal violet was fully washed with sterilized PBS. Then, the biofilm was fully decolorized with 95% ethanol. The mixture of ethanol and crystal violet was absorbed and transferred to a new 96-well plate, and the optical density was measured at 570 nm.

Propidium Iodide (PI)

The spore suspension of 3×10^5 CFU/mL was inoculated with a 6-well plate, and a layer of hyphae was formed later on incubation in a constant temperature incubator (37 °C, 5% CO_2) for 24 h. Different concentrations (32 and 64 μg/mL) of ZIF-90 were covered on the surface of hyphae. The incubation continued for 24 h, and then the culture solution was sucked out. The hyphae were washed 3 times with sterile PBS and then stained with PI staining solution (Solarbio, Beijing, China). Then, the hyphae were incubated for 15 min and protected from light. The hyphae were photographed with a fluorescence microscope (Nikon, Tokyo, 200×).

Calcofluor White Stain (CFW; Sigma)

A spore suspension of 3×10^5 CFU/mL was co-cultured with ZIF-90 in a 12-well plate for 24 h. The 12-well plate was washed 3 times with sterile PBS. The Calcium Fluoride White Stain was added to the 12-well plate. Then, the plate was incubated for 15 min at room temperature, avoiding light. The fluorescence intensity was observed under a fluorescence microscope (Nikon, Tokyo, 200×) and photographed.

Hyphae Scanning Electron Microscopy (SEM)

A 3×10^5 CFU/mL spore suspension was inoculated with a 6-well plate. A layer of hyphae was formed after 24 h of incubation in a constant temperature incubator (37 °C, 5% CO_2), and ZIF-90 (64 μg/mL) was covered on the surface of the hyphae. The incubation continued for 24 h. Next, the hyphae were washed 3 times with sterile PBS and fixed with

2.5% glutaraldehyde solution. The hyphae morphology was observed under a scanning electron microscope (JSM-840; JOEL, 200×).

Cell Culture and Hyphae Stimulation

RAW 264.7 cells were cultured in DMEM high sugar medium (Biological Industries, Israel) supplemented with 10% fetal bovine serum. RAW 264.7 cells in cell culture plates were stimulated with *A. fumigatus* filaments for 1 h. Then ZIF-90 was added, and the stimulation continued for 8 h or 24 h. Cells were incubated in a constant temperature incubator (37 °C, 5% CO_2).

Annexin V-FITC/ PI Apoptosis Staining (E-CK-A211, Elabscience)

RAW 264.7 cells were inoculated in 12-well plates, and subsequently, the cell density grew to 1×10^5, and inactivated hyphae were added to stimulate the cells for 1 h. Afterward, ZIF-90 (64 μg/mL) was added to treat the cells for 24 h. Cells were collected and suspended with 500 of diluted 1×Annexin V Binding Buffer. 5 μL of Annexin V-FITC Reagent and 5 μL of PI Reagent were added to the cell suspension, and the cells were incubated at room temperature and protected from light for 15–20 min then were detected by a flow cytometer (Agilent NovoCyte 2060R) within 1 h.

Apoptosis Fluorescence Hoechst Staining (C0021, Solarbro)

RAW 264.7 cells were inoculated in 12-well plates. When the cell density reached 1×10^5, inactivated hyphae were added to stimulate for 1 h. Then, ZIF-90 (64 μg/mL) was added to continue the incubation for 8 h. The 12-well plate was washed with PBS, and then a PBS and Hoechst staining solution were added. The 12-well plate was placed in the refrigerator at 4 °C for 20–30 min. The photographs of stained cells were taken under a fluorescence microscope (EVOS M5000, Thermo; 400×).

Mitochondrial Reactive Oxygen Species Detection

MitoSOX Red, a fluorescent probe for mitochondrial superoxide, is specifically oxidized by superoxide after penetrating the mitochondria, generating red fluorescence, thus marking mtROS. For experimental use, MitoSOX Red was prepared by diluting in a serum-free medium to achieve a final concentration of 100 nmol/L.

RAW 264.7 cells were preincubated with medium supplemented with ZIF-90 (64 μg/mL) or DMSO as a control for 2 h in 24-well plates. After incubation, the cells were rinsed 3 times with PBS and then exposed to *A. fumigatus* hyphae for 8 h.

The cells were washed again with PBS, followed by the addition of 500 μL MitoSOX Red solution to each well and incubation for 20 min at room temperature. After staining with MitoSOX Red, the cells were thoroughly rinsed with PBS, and 20 μL DAPI solution was added to each well for nuclear counterstaining under light-protected conditions for 10 min. The treatment of *A. fumigatus* is the same as above. Finally, the cells were washed 3 times with PBS, and fluorescence images were captured using a fluorescence microscope (EVOS M5000, Thermo; 200×).

Corneal Toxicity Test

The toxicity of ZIF-90 to the mouse cornea was investigated based on an ocular toxicology study (Draize Toxicity Assay).[25] The right eye of mice was treated with DMSO or ZIF-90 (5 μL once a day; 0.1% DMSO, 64 and 128 μg/mL of ZIF-90), and the left eye served as a blank control. Fluorescence staining (CFS) of the corneas of mice on days 1, 3, and 5 was observed under cobalt blue light to reflect the toxicity of ZIF-90 to the mouse cornea. The area and density of corneal ulcers, iritis, and conjunctival erythema were scored.

Establishment and Treatment of Mice Keratitis Model

Mice (female C57BL/6 mice 6–8 weeks, 20–30 g weight) were narcotized with 8% chloral hydrate. *A. fumigatus* conidial suspension (2 μL,3×10^7 CFU/mL) was later injected into the corneal stroma, and the left eye was used as a blank control group without treatment.[26] Processing is in accordance with the Association for Research in Vision and Ophthalmology (ARVO) Statement for the Use of Animals in Ophthalmic and Vision Research.

Mice with fungal keratitis were treated by subconjunctival injection of 5 μL of ZIF-90 (64 and 128 μg/mL) or DMSO (0.1%) once daily for 5 days. The progression of keratitis in mice was recorded with a camera under a slit lamp and scored clinically according to a 12-point scoring guideline.

HE Staining

Eyeballs of mice infected with fungal keratitis were taken after 3 days of infection. The eyeballs were fixed for 48 h and then embedded in paraffin and sectioned (thickness of 10 μm). The sections were stained with hematoxylin and eosin stains. Then, the sections were photographed and recorded under a light microscope (Axio Vert; Zeiss, Jena, Germany, 400×).[27]

Immunofluorescence (IF)

The eyeballs of mice were taken and placed in an OCT embedding agent. The slices (10 μm) of the eyeballs were cut by freezing microtome upon the completion of quick freezing with liquid nitrogen. The slices were attached to adhesion pathology slides and roasted in an incubator at 37 °C for 8 h. Then, the specimens were fixed with methanol. Once fixed, it was soaked with PBS. The sample was dried and sealed with goat serum. Then, the specimen was incubated with NIMP-R14 antibody (1:100, Invitrogen) overnight (4 °C). The tablets were incubated for 1 h with the second antibody (FITC-conjugated) and finally sealed with anti-fluorescence attenuation tablets after 10 min of DAPI incubation. Images were photographed under fluorescence microscope (400x).

Quantitative Real-Time PCR Experiments (RT-PCR)

RAW 264.7 cells were inoculated in 12-well plates. When cells grew to 80%-90% of the well plate area, they were stimulated with inactivated *A. fumigatus* filaments for 1 h. The cells were treated with ZIF-90 (64 μg/mL) for 8 h. The cells were treated with ZIF-90 (64 μg/mL) for 8 h. Total ribonucleic acid (RNA) was collected to check for inflammatory factors IL-6, TNF-α, and IL-1β.

The corneas of mice at 3-day and 5-day postinfection (p.i.) were collected. Total RNA was collected, and inflammation-related factors IL-6, IL-1β, and TNF-α were examined by the same procedure as above. The inflammatory factors primers sequence of mice can be found in Table 1.

Enzyme-Linked Immunosorbent Assay (ELISA)

The supernatant of RAW 264.7 cells was taken and placed in PBS containing phenyl methyl sulfonyl fluoride (PMSF; Solarbio). Corneal tissue was crushed using a TissueLyser (QIAGEN, China). Next, the level of inflammatory protein in the supernatant was detected by an ELISA kit (Biolegend, CA, USA). Protein concentration was determined by absorbance at 450 nm.

Results and Discussion

Synthesis and Characterization of ZIF-90

We successfully synthesized ZIF-90 with zinc nitrate and ICA (Figure 1A). The SEM characterization of ZIF-90 disclosed uniform and well-defined crystalline morphology (Figure 1B). The particles of ZIF-90 exhibited a regular

Table 1 Nucleotide Sequences of Mice Primers for RT-PCR

Gene	GenBank No.	Primer Sequence (5' - 3')
GAPDH	NM_008084.2	F: AAATGGTGAAGGTCGGTGTG R: TGAAGGGGTCGTTGATGG
IL-1β (mouse)	NM_008361.3	F: CGC AGC AGC ACA TCA ACA AGA GC R: TGT CCT CAT CCT GGA AGG TCC ACG
IL-6 (mouse)	NM_001314054.1	F: TGA TGG ATG CTA CCA AAC TGG A R: TGT GAC TCC AGC TTA TCT CTT GG
TNF-α (mouse)	NM_013693.2	F: ACCCTCACACTCAGATCATCTT R: GGTTGTCTTTGAGATCCATGC

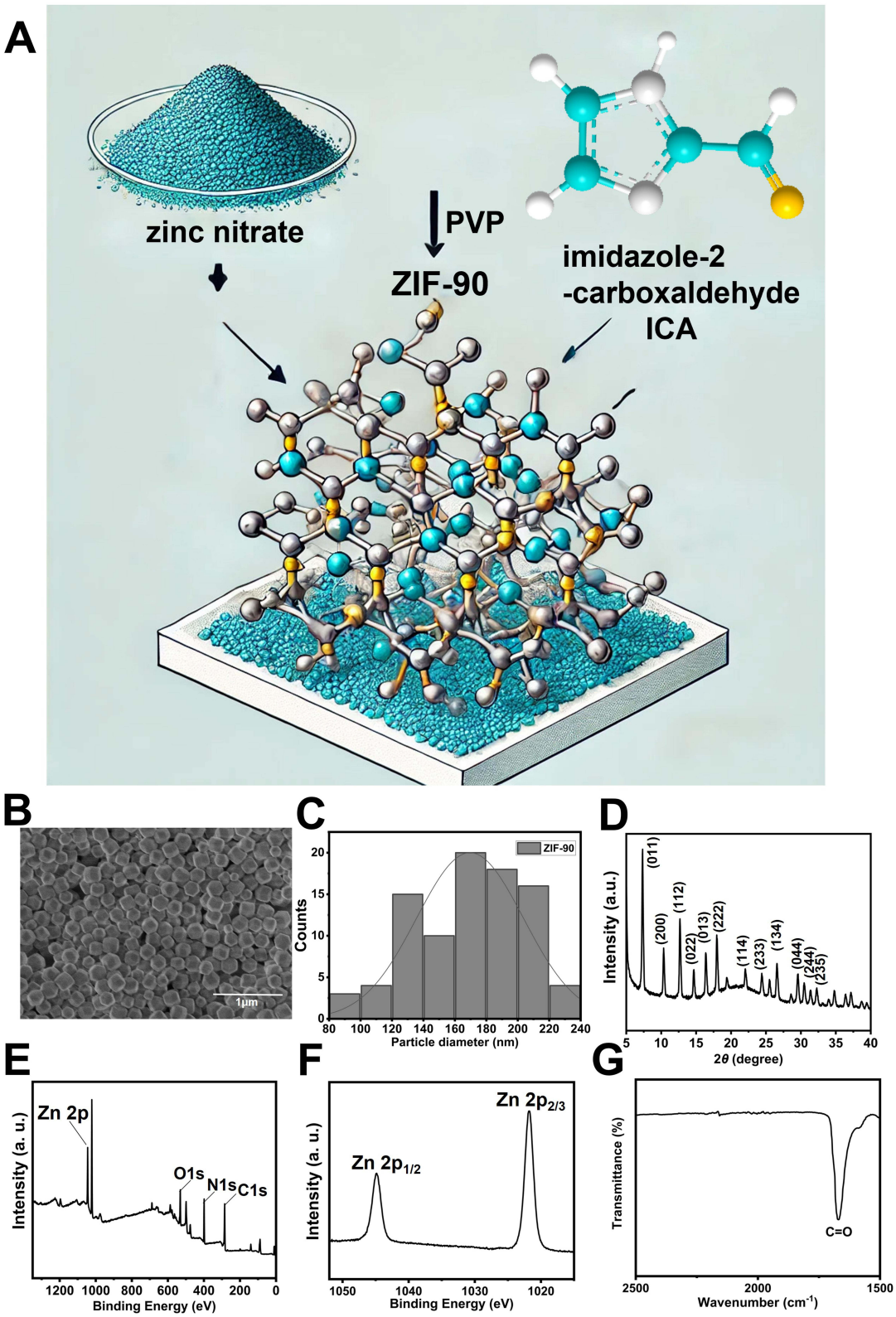

Figure 1 Synthesis and characterization of ZIF-90 (**A**) Diagram of the synthesis process of ZIF-90 (**B**) SEM detection of ZIF-90 (Scale bar: 1μm) and (**C**) Particle size distribution graph of ZIF-90 (**D**) XRD pattern of ZIF-90 (**E**) XPS graphs (**F**) XPS graphs for Zn 2p (**G**) FT-IR maps of ZIF-90 can demonstrate the presence of aldehyde groups.

https://doi.org/10.2147/IJN.S517169

shape and size distribution, indicating high-quality synthesis. The average size of ZIF-90 particles was 170 nm (Figure 1C). The XRD analysis further confirmed the crystalline structure of ZIF-90, displaying distinct diffraction peaks that align with the expected pattern of the ZIF-90 framework (Figure 1D). XPS was employed to analyze the surface composition and chemical states of the elements present in ZIF-90. The survey spectrum revealed distinct peaks corresponding to zinc (Zn 2p, 1022.7 eV), carbon (C 1s, 248.8 eV), nitrogen (N 1s, 398.4 eV), and oxygen (O 1s, 531.1 eV), indicating the presence of ZIF-90 (Figure 1E). The high-resolution Zn 2p spectrum revealed characteristic peaks at approximately 1022 eV ($Zn\ 2p_{1/2}$) and 1045 eV ($Zn\ 2p_{3/2}$), confirming the coordination of zinc in the ZIF-90 framework (Figure 1F). The prominent peak around 1700 cm^{-1} in the FT-IR spectrum indicates the presence of the aldehyde group (–CHO), which is a key feature distinguishing ZIF-90 from other ZIFs (Figure 1G). These results validated the successful synthesis of ZIF-90.[28]

Cytotoxicity in Vitro and Anti-A. Fumigatus Properties of ZIF-90

In order to verify whether ZIF-90 can be used on HCECs and macrophages (RAW 264.7 cells), this test was conducted using a cytotoxicity assay (CCK-8). The result of CCK-8 illustrated that ZIF-90 was non-toxic to both HCEC cells and RAW 264.7 cells at a concentration of 128 μg/mL or less (Figure 2A and B). The safe concentration of ZIF-90 for HCECs and RAW 264.7 cells in vitro is no more than 128 μg/mL.

The spore adhesion experiment exhibited that ZIF-90 significantly reduced the adhesion of *A. fumigatus* spores to corneal epithelial cells (Figure 2C and D). The number of spores attached to the HCECs indicated that the number of spores in the ZIF-90 group was significantly lower than that in the control group (Figure 2E, $p<0.0001$). The conidia attached to the corneal epithelium then germinated into mycelia. This process releases toxins and enzymes, triggering an uncontrollable immune response and inflammation. These reactions may eventually lead to irreversible corneal damage.[29,30] ZIF-90 inhibited the adhesion of spores to corneal epithelial cells, which helps to reduce the occurrence of host immune response and inflammatory response, thereby reducing the irreversible damage to the cornea.

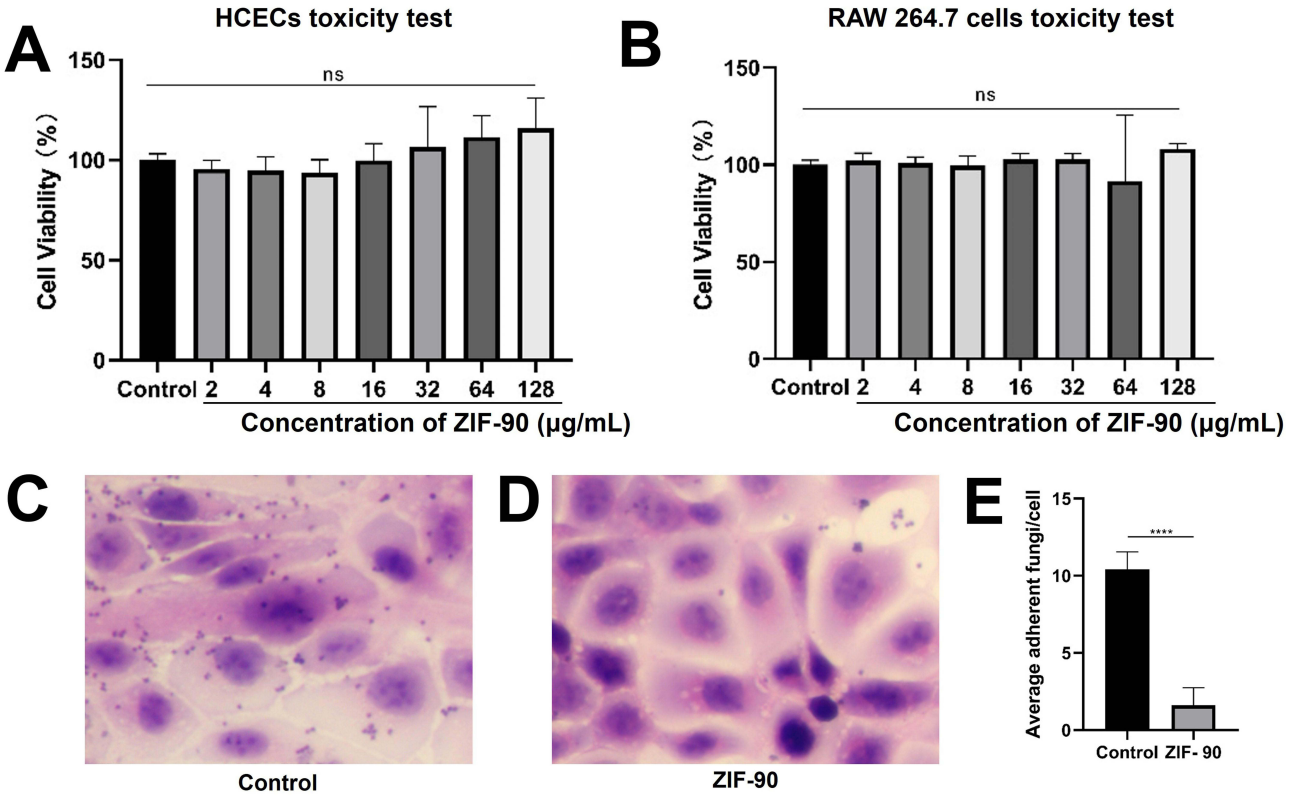

Figure 2 Cells cytotoxicity and anti-adhesion of *A. fumigatus* spores by ZIF-90. Effects of different ZIF-90 concentrations on (**A**) HCECs and (**B**) RAW 264.7 cells upon finishing incubation for 24 h, ZIF-90 (2–128 μg/mL). The adhesion of *A. fumigatus* to HCECs separately added (**C**) DMSO and (**D**) ZIF-90. And (**E**) the statistical quantitative analysis of spore adhesion (ns, no significance, **** $p<0.0001$).

To further explore the effect of ZIF-90 on *A. fumigatus*, we conducted a series of experiments, including spore adhesion test, MIC, biofilm inhibition test, PI, and calcium fluoride white staining. The MIC results displayed that ZIF-90 inhibited the formation of *A. fumigatus* at 32 μg/mL (Figure 3A, $p<0.0001$) and inhibited the formation of more than 90% *A. fumigatus* hyphae at the concentration of 64 μg/mL.

The biofilm inhibition experiment showed that ZIF-90 can suppress the biofilm formation of *A. fumigatus* at 16 μg/mL. More than 90% of biofilm formation was inhibited by ZIF-90 at 64 μg/mL (Figure 3B, $p<0.0001$). Biofilm formation is one of the main mechanisms of fungal resistance formation. The production of fungal cell biofilm played a crucial role in fungal resistance to clinical drugs. Inhibition of biofilm is conducive to preventing the formation of resistance to *A. fumigatus*.[31–33]

The SEM (Figure 3C and D) presented that the addition of ZIF-90 (Figure 3D) destroyed the fluency and integrity of *A. fumigatus* hyphae in comparison to the hyphae that only added DMSO (Figure 3C). PI staining indicated that compared with the control group (Figure 3E), the hyphae membrane of *A. fumigatus* in the ZIF-90 group was significantly damaged (Figure 3F and G). Calcium fluoride white stain was used to assess the changes in the cell wall (Figure 3H–J). Compared with the control group (Figure 3H), no fungal hyphal cell wall was observed after adding different concentrations of ZIF-90 (Figure 3I–J). Fungal cell walls and membranes are crucial in maintaining cell homeostasis and protecting cell stability. The above experiments demonstrated that ZIF-90 affected the homeostasis of fungal cells.

Antifungal and biofilm-inhibitory mechanisms of zinc ions (Zn^{2+}) and imidazole groups in ZIF-90 exhibit several noteworthy effects. Firstly, Zn^{2+} ions exert antifungal activity by disrupting zinc-dependent enzymatic functions within fungal cells, leading to metabolic inhibition and cell death. Additionally, Zn^{2+} ions compromise fungal cell membrane integrity, increasing permeability and causing leakage of vital cellular components. Moreover, Zn^{2+} induces oxidative stress by generating reactive oxygen species (ROS), which damage critical cellular structures, including lipids, proteins, and DNA.[34]

ZIF-90 serves a key function in inhibiting fungal biofilm formation. They interfere with the synthesis of the extracellular matrix, a key component of biofilms, and disrupt quorum sensing, which is essential for biofilm development. Furthermore, imidazole groups may integrate into fungal cell membranes, altering their fluidity and reducing the ability of fungal cells to adhere to surfaces, thus preventing biofilm formation.[21,35,36]

The synergistic effect of zinc ions and imidazole groups within ZIF-90 significantly enhances antifungal efficacy by targeting multiple cellular mechanisms simultaneously. This combined action disrupts key processes within fungal cells, leading to improved antifungal performance. These findings illustrate the potential of ZIF-90 as a promising candidate for antifungal therapies, particularly in preventing biofilm-associated infections. Previous studies have demonstrated the antifungal efficacy of the metronidazole and ZIF-90 composite.[14] Our experimental results suggest that ZIF-90, while acting as a vector, may also play an antifungal role.

ZIF-90 Promotes Apoptosis of Macrophages and Reduces Inflammation

Annexin V-FITC/PI apoptosis staining and Hoechst apoptosis staining were two classical methods for examining apoptosis. We verified the effect of ZIF-90 on the apoptosis of RAW 264.7 cells.

Annexin V is a calcium-dependent phospholipid-binding protein with a high affinity for phosphatidylserine (PS). The combination of PI and Annexin V can distinguish cells at different stages of apoptosis. Annexin V-FITC and PI double-positive cells are apoptotic cells. The results manifested that compared with the control group, treatment with hyphae stimulation alone, hyphae stimulation plus DMSO, and the addition of ZIF-90 (32 μg/mL) on the completion of hyphae stimulation did not promote the apoptosis of macrophages. The treatment with ZIF-90 (64 μg/mL; Figure 4A–E) significantly increased (Figure 4F, $p<0.01$) the number of apoptotic macrophages, proving that ZIF-90 can promote macrophage apoptosis.

When cells undergo apoptosis, chromatin shrinks. Hoechst dye can penetrate the cell membrane, and the fluorescence of apoptotic cells is markedly enhanced than that of normal cells following staining. Our results highlighted that compared with the fungal stimulation alone group (AF, Figure 4G), the fluorescence of the group supplemented with ZIF-90 in succession to fungal stimulation was significantly enhanced (ZIF-90, Figure 4G). Besides, we conducted quantitative and statistical

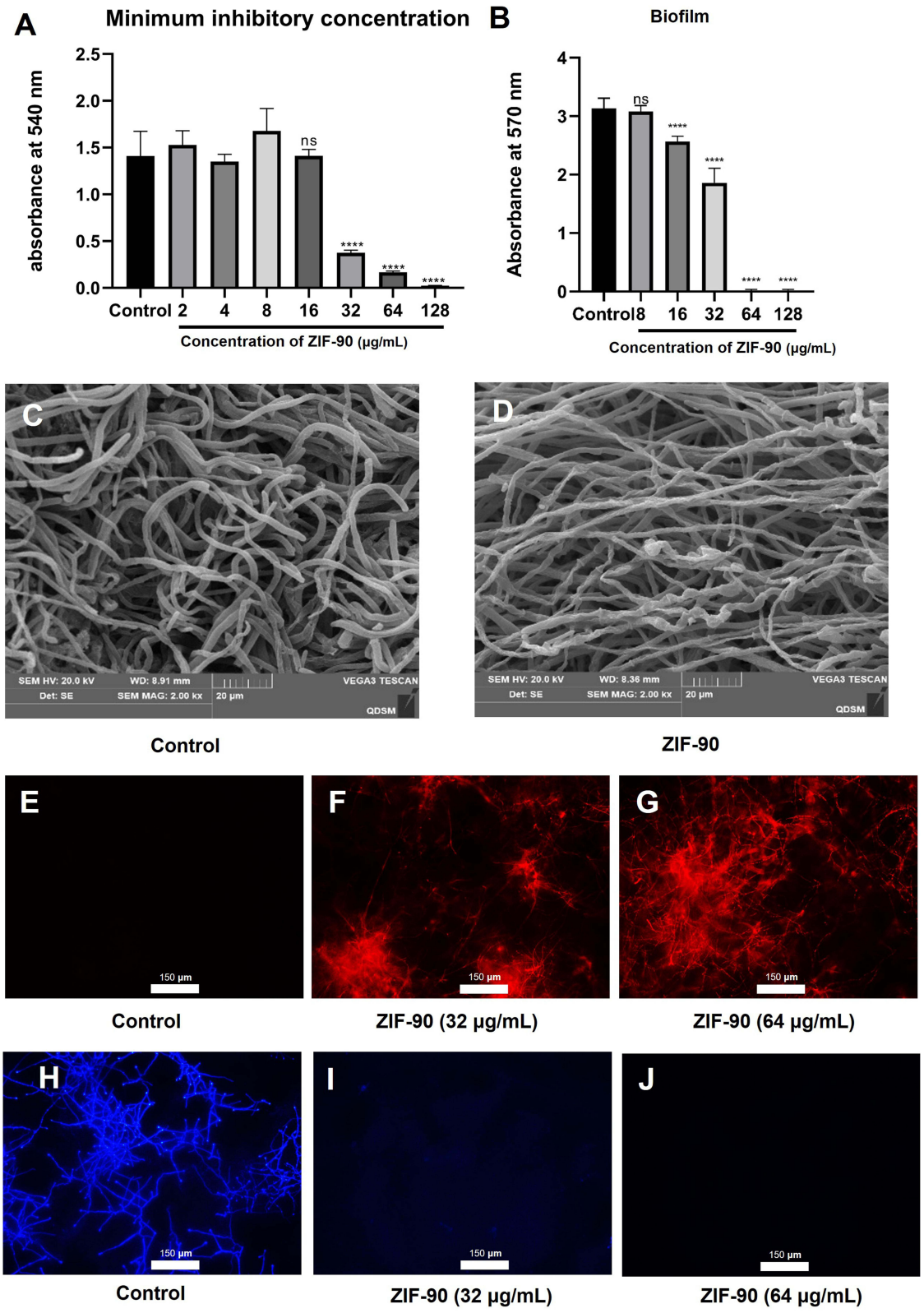

Figure 3 Anti-*A. fumigatus* action of ZIF-90 (**A**) Inhibiting the growth of *A. fumigatus* with different concentrations of ZIF-90, ZIF-90 (2–128 μg/mL). (**B**) Influence of ZIF-90 on inhibiting the growth of *A. fumigatus* biofilm, ZIF-90 (8–128 μg/mL). (**C** and **D**) Effect of ZIF-90 on mycelial morphology and structure of *A. fumigatus*, ZIF-90 (64 μg/mL). Impact of various ZIF-90 concentrations on the fungal cell membrane. (**E**–**G**) integrity and cell wall. (**H**–**J**) structure, ZIF-90 (32 and 64 μg/mL). (ns, no significance, **** $p<0.0001$).

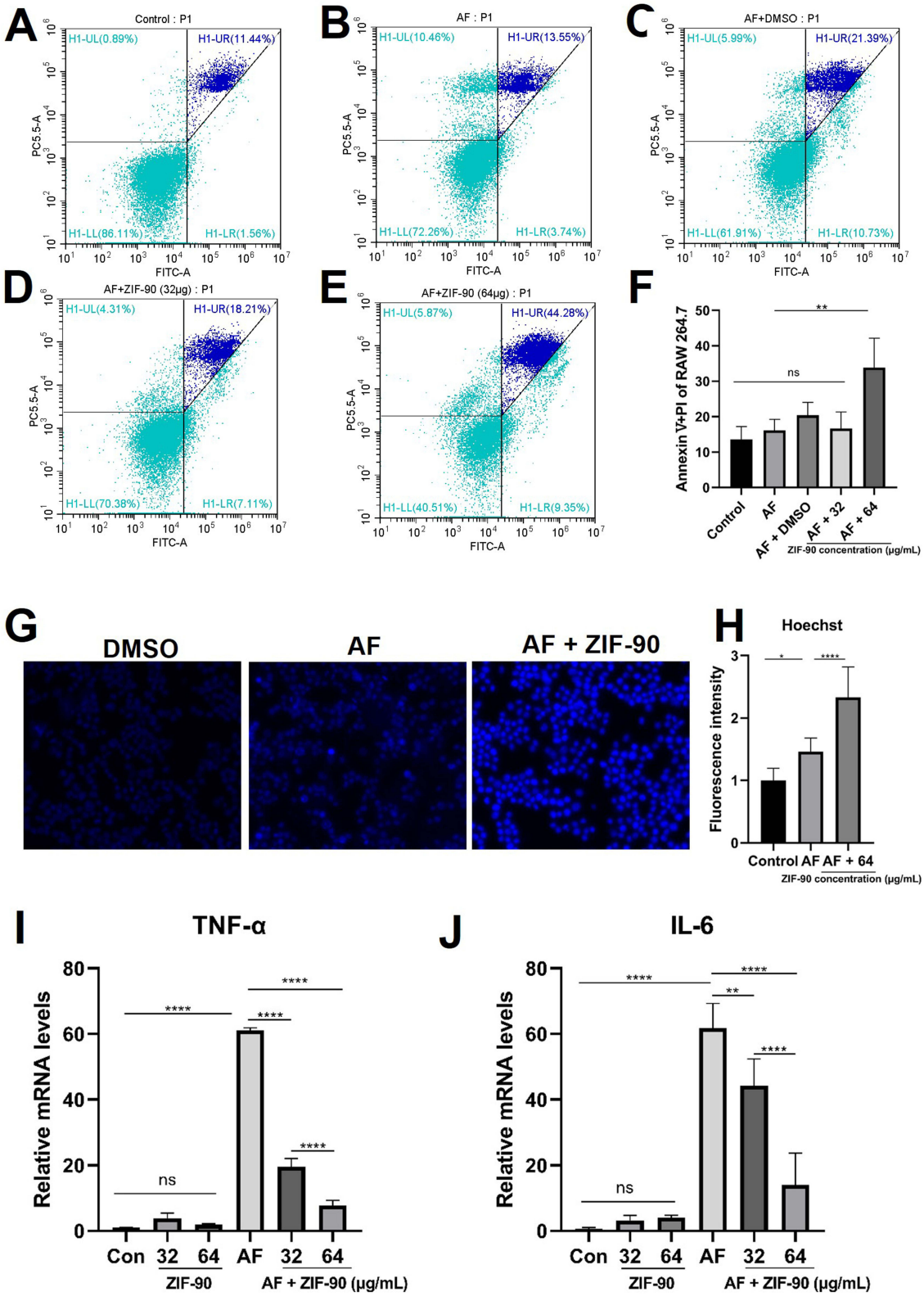

Figure 4 ZIF-90 affects RAW 264.7 cells apoptosis. (**A**–**E**) Flow cytometry depicted that ZIF-90 (64 μg/mL) could promote the apoptosis of RAW 264.7 cells post *A. fumigatus* infection labeled with Annexin V and PI. (**F**) Statistical analysis of RAW 264.7 cells apoptosis rate dyed by Annexin V and PI. Hoechst staining and statistical quantitative analysis of RAW 264.7 cells (**G**) showed that ZIF-90 (64 μg/mL) could promote apoptosis (**H**). The changes of pro-inflammatory factors TNF-α (**I**) and IL-6 (**J**). (ns, no significance; * p<0.05, ** p<0.01, **** p<0.0001).

https://doi.org/10.2147/IJN.S517169

analysis of different groups and found that the fluorescence intensity of apoptotic macrophages in the ZIF-90 treatment group was indeed higher than that in the AF group (Figure 4H, $p<0.0001$). This result further confirms that ZIF-90 can promote macrophage apoptosis. In addition, through the changes of inflammatory factors, we can see that when the concentration of ZIF-90 increases from 32 μg/mL to 64 μg/mL, the contents of pro-inflammatory factors TNF-α (Figure 4I) and IL-6 (Figure 4J) are significantly decreased ($p<0.0001$) and the anti-inflammatory effect is significantly increased. These results suggest that ZIF-90 can further control inflammation by promoting apoptosis of macrophages.

Macrophages have a significant impact on the immune response to fungal keratitis by producing pattern-recognition receptors to clear the invading fungus. Excessive immune and inflammatory responses can damage the corneal epithelium and decrease vision.[6,8,37] Hence, the regulation of macrophage survival and its production of inflammatory factors are pivotal in the protection of corneal cells. Apoptosis is a regulated and controlled process that contributes importantly to maintaining homeostasis and tissue development by eliminating damaged, unnecessary, or potentially harmful cells without triggering an inflammatory response. Besides, it has been demonstrated that apoptotic macrophages can release specific anti-inflammatory substances while maintaining the integrity of the plasma membrane.[38] Thus, we investigated the effect of ZIF-90 on macrophage apoptosis. Accordingly, it can be concluded that ZIF-90 can promote apoptosis of macrophages, and the effect of ZIF-90 on reducing inflammatory factors is through promoting apoptosis of macrophages.

ZIF-90 Increased Mitochondrial mtROS of A. Fumigatus and Decreased mtROS Levels of RAW 264.7 Cells

The experiment employed the MitoSOX Red probe to assess ROS levels in the mitochondria of A. fumigatus, as illustrated in Figure 5A and B. Compared to the control group, both 32 μg/mL and 64 μg/mL concentrations of ZIF-90 significantly elevated the MitoSOX fluorescence signal in *A. fumigatus*, particularly in the 64 μg/mL group, where fluorescence intensity increased by approximately sixfold (Figure 5B). These findings suggest that ZIF-90 can exert oxidative stress on A. fumigatus by inducing mitochondrial ROS production, ultimately leading to fungal metabolic dysregulation and even cell apoptosis.

This phenomenon may be attributed to the structural characteristics of ZIF-90, as its metal-organic framework may interfere with fungal mitochondrial function. The ROS elevation triggered by ZIF-90 further verifies its underlying antifungal activity mechanism, providing theoretical support for its potential as an antifungal agent.

In a model of RAW 264.7 macrophages infected with A. fumigatus, ZIF-90 demonstrated the ability to reduce host mitochondrial ROS production (Figure 5C). ROS levels were significantly elevated in the infected RAW 264.7 cells, but upon the addition of 64 μg/mL ZIF-90, the MitoSOX fluorescence signal was significantly reduced, returning to levels close to those of the control group (Figure 5D). This result indicates that ZIF-90 can alleviate the oxidative stress induced by infection, potentially preserving host cell function and reducing inflammatory damage.

The reduction of mtROS levels in macrophages contributes to limiting excessive inflammatory responses, thereby protecting host tissues. Conversely, an increase in mtROS levels in fungi disrupts their metabolic balance and impairs their survival ability, presenting a therapeutic target for the host. This provides a theoretical basis for utilizing mtROS modulation as a potential strategy for treating infections.[10,11,39]

Verification of Corneal Toxicity of ZIF-90 in Mice

The important prerequisite for the application of the drug in the eyes of mice is that the drug is non-toxic to the corneal epithelium of mice. The results presented that no corneal defect was observed under cobalt blue light at 0, 1, 3, and 5 days after the eye subconjunctival injection (Figure 6A). Additionally, the score of corneal fluorescein sodium staining was found to be 0 score both in the control group and ZIF-90 treatment group at different concentrations (64 and 128 μg/mL) at days 0, 1, 3, and 5 (Figure 6B). To summarize, ZIF-90 of 64 and 128 μg/mL had no potential toxicity to the corneal epithelium of mice. The results manifest that ZIF-90 was non-toxic to the ocular surface of mice and could be used to treat fungal keratitis in mice.

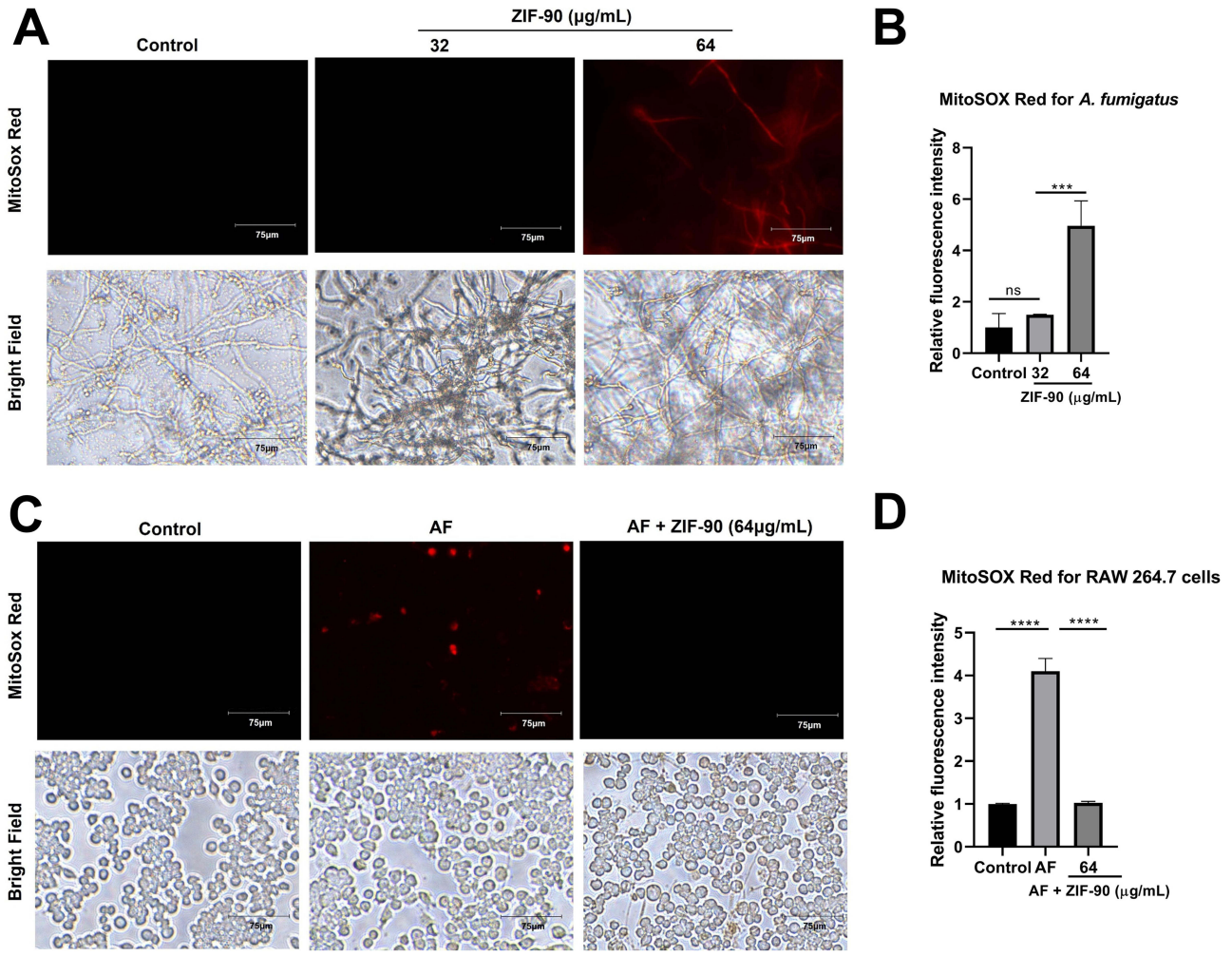

Figure 5 Regulatory effects of ZIF-90 on mitochondrial ROS levels in *A. fumigatus* and RAW 264.7 cells. MitoSOX Red fluorescent staining shows the effect of ZIF-90 on mitochondrial ROS levels in *A. fumigatus* (**A**), along with quantitative analysis of fluorescence intensity (**B**). In a model of *A. fumigatus* infection in RAW 264.7 cells, MitoSOX Red fluorescent staining results after ZIF-90 (64 μg/mL) treatment (**C**) and quantitative analysis of fluorescence intensity (**D**). (ns, no significance, *** p<0.001, **** p<0.0001).

ZIF-90 for the Treatment of Mouse A. Fumigatus Keratitis

Ocular anterior segment photographs of mice with fungal keratitis were captured using a slit lamp. In the PBS control group, corneal opacity, ulceration, and epithelial defects were evident at 3 days of *A. fumigatus* infection, with an escalation in the severity of the infection observed in the corneas later on 5 days (Figure 6C). The corneas treated with ZIF-90 exhibited slight structural damage and a reduction in opacity. Additionally, clinical evaluations demonstrated significantly lower scores (Figure 6D) in the ZIF-90 group, indicating improved therapeutic outcomes. Therefore, it is established that ZIF-90 has the effect of treating fungal keratitis.

Imidazole derivatives, which form the core structure of various antifungal agents (eg, ketoconazole and miconazole), exert their effects by inhibiting the biosynthesis of ergosterol. Disruption of ergosterol compromises membrane integrity could lead to increased permeability and eventual fungal cell lysis. Zinc ions (Zn^{2+}) also contribute to antifungal activity by interfering with fungal metabolic processes, inhibiting key enzymes involved in fungal growth, and destabilizing fungal biofilm structures. Furthermore, zinc ions impede fungal spore germination and hyphal development, thereby preventing fungal colonization.[40–42] This makes them a promising strategy of ZIF-90 for treating persistent fungal infections, including fungal keratitis.

https://doi.org/10.2147/IJN.S517169

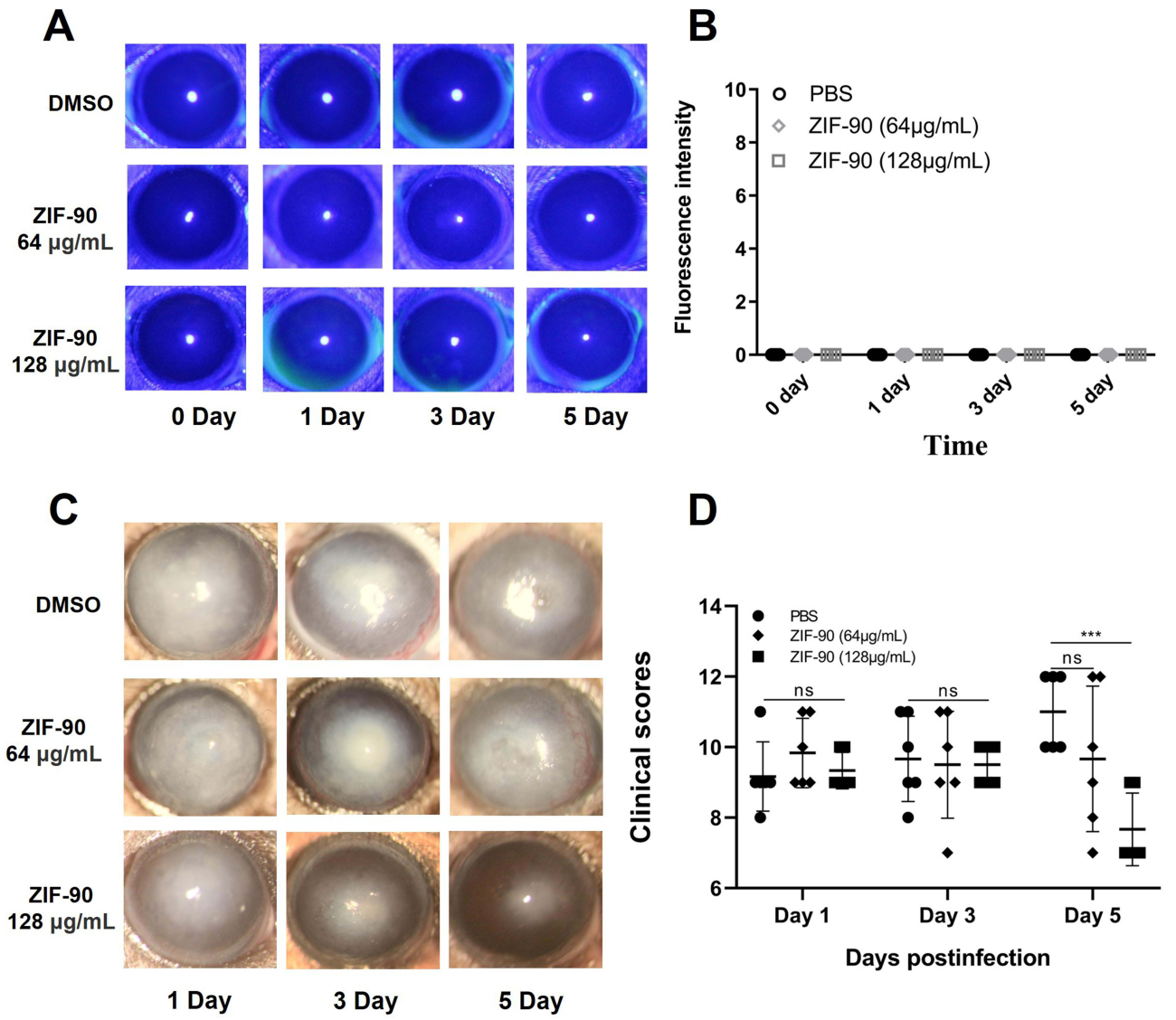

Figure 6 Corneal toxicity of ZIF-90 and therapeutic effect of ZIF-90 on fungal keratitis in mice. Fluorescein sodium staining of mice cornea using ZIF-90 (**A**) and fluorescence intensity (**B**) succeeding staining. Therapeutic effect (**C**) and clinical score (**D**) of ZIF-90 in mice with fungal keratitis. (ns, no significance; *** p<0.001).

Corneal Cell Inflammatory Changes and Anti-Inflammatory Effect of ZIF-90

The control of inflammatory response is a crucial indicator for the effective treatment of fungal keratitis. The down-regulation of inflammatory cell infiltration can imply the inflammatory response is well controlled. HE staining showed that ZIF-90 decreased the content of inflammatory cells in corneal tissues infected with fungal keratitis (Figure 7A). Neutrophils are the most abundant inflammatory cells in the early stage of fungal keratitis. Immunofluorescence staining denoted the content of neutrophils in the cornea of mice infected with *A. fumigatus* after ZIF-90 treatment also decreased (Figure 7B). As well we verified that the pro-inflammatory factors IL-1β, IL-6, and TNF-α in the cornea of mice treated with ZIF-90 were significantly reduced on the 3 and 5 days p.i. compared with those treated with PBS (Figure 7C–E).

Excessive infiltration of inflammatory cells during the development of fungal keratitis contributes to significant corneal tissue damage.[43] Neutrophils and macrophages release pro-inflammatory cytokines and ROS, which not only target the fungal infection but also lead to corneal stromal degradation, ulceration, and opacity.[44] This results in impaired wound healing and, in severe cases, corneal perforation, causing vision impairment. Effective treatment requires careful management of the immune response to avoid exacerbating inflammation and tissue damage. Treatment with ZIF-90 effectively controlled the immune response and avoided increased inflammation and tissue damage. In addition,

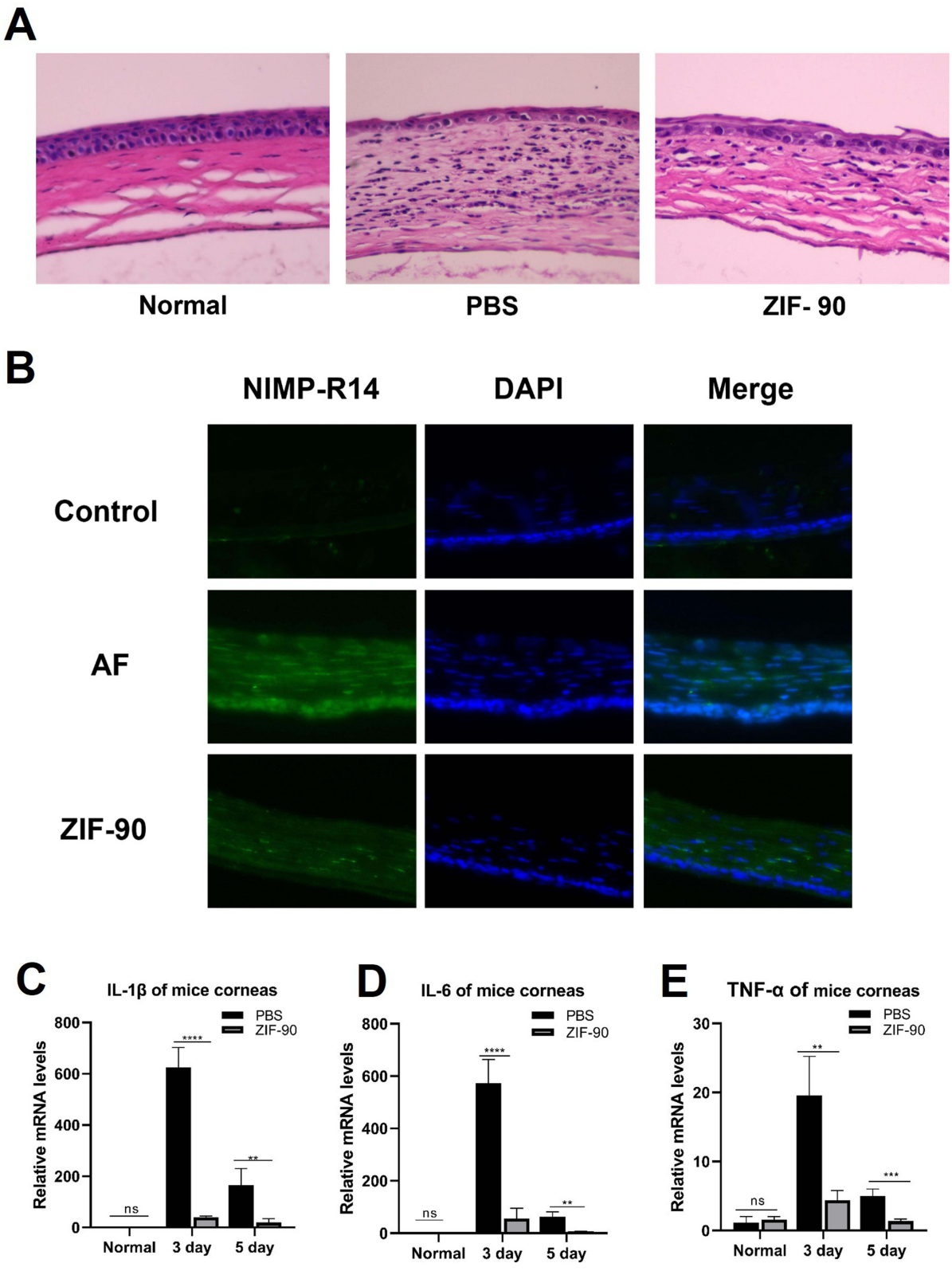

Figure 7 Changes of corneal inflammatory cells and inflammatory factors in mice (**A**) HE staining reflected the penetration of inflammatory cells in different groups of mice three days in line with infection. (**B**) Fluorescent staining of neutrophil infiltration in mice infected with fungal keratitis. Infiltration of corneal inflammatory factors (**C**) IL-1β, (**D**) IL-6, and (**E**) TNF-α in mice. (ns, no significance; ** p<0.01, *** p<0.001, **** p<0.0001).

https://doi.org/10.2147/IJN.S517169

imidazole antifungal drugs are also known to have anti-inflammatory effects.[45,46] Therefore, the administration of ZIF-90, aimed at improving the inflammatory response in fungal keratitis, combined with imidazole antifungal drugs, may represent a highly effective treatment option for fungal keratitis.

Cytotoxicity, Antifungal and Anti-Inflammatory Effects of ZIF-8, ZIF-67 and MOF-74

In order to endorse the effective antifungal components in ZIF-90 and to judge the biocompatibility of ZIF-90, we identified ZIF-8, ZIF-67, and MOF-74 (Zn) with different metal ion compositions and different organic ligands from ZIF-90. ZIF-8 differs from ZIF-90 by an aldehyde group. ZIF-67 differs from ZIF-90 by an aldehyde group (-CHO) and zinc ions. MOF-74 (Zn) shares zinc ions with ZIF-90 but has different organic ligands. These three MOF materials are also widely used as carriers in the biomedical field.[47–51] While verifying the antifungal component of ZIF-90, it is also possible to certify the antifungal potential of other MOF materials to expand the application field of MOF materials.

To study the cytotoxicity of these materials, the cellular activity of HCECs and RAW 264.7 cells was detected by the CCK-8 kit. The results indicated that ZIF-90 was non-toxic to both HCECs and RAW 264.7 cells at concentrations less than 128 μg/mL (Figure 2A–B). The other three materials were toxic to HCECs and RAW 264.7 cells at 64 μg/mL (Figure 8A–F), and MOF-74 (Zn) was toxic to RAW 264.7 cells at 32 μg/mL (Figure 8F, $p<0.0001$). Compared to ZIF-8, ZIF-67, and MOF-74 (Zn), ZIF-90 exhibited better biocompatibility, reflecting lower cytotoxicity. Since the difference between ZIF-90 and ZIF-8 was only in the structure of the aldehyde group and a hydroxyl group, we manifest that the presence of the aldehyde group is conducive to reducing the toxicity of ZIF materials.

MIC experiment results illustrated that MOF-74 (Zn) has the ability to block the growth of *A. fumigatus* at 16 μg/mL (Figure 8A, $p<0.0001$). At 32 μg/mL, ZIF-8, ZIF-67, MOF-74 (Figure 9A–C, $p<0.0001$) and ZIF-90 (Figure 3A) all inhibited fungal growth. When the concentration reached 64 μg/mL, ZIF-8, MOF-74 (Figure 9A–B), and ZIF-90 (Figure 3A) could impede more than 80% of the fungal growth. The antifungal rate of these three materials exceeded 90% at 128 μg/mL. However, the inhibition rate of ZIF-67 could not reach 80% even at a concentration of 128 μg/mL (Figure 9C, $p<0.0001$). Although these four MOF materials have good anti-fungal effects, the effect of ZIF-67 is not as good as the other three materials. In these four MOF materials, ZIF-67 is the only MOF material whose metal ions are

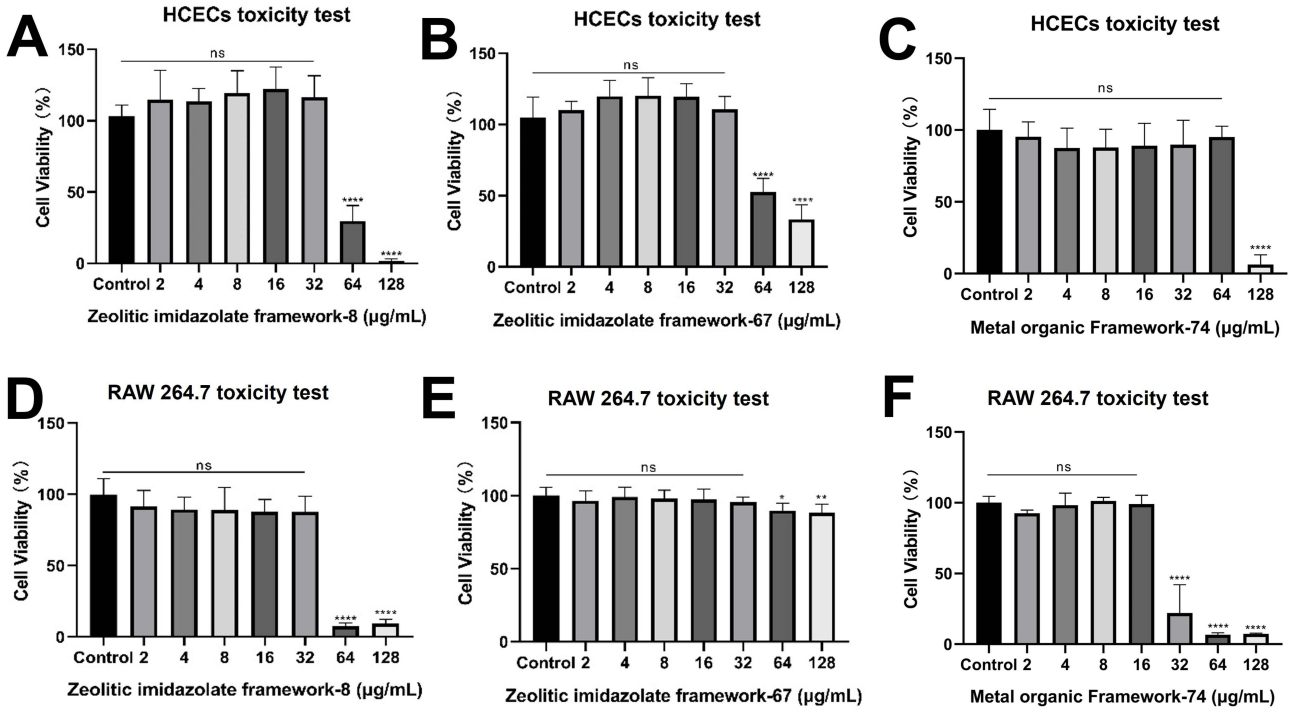

Figure 8 Poisonousness of different MOF materials to different cells. Toxicity of materials at different levels of (**A**) ZIF-8, (**B**) ZIF-67, and (**C**) MOF-74 to HCECs. And Cytotoxicity of (**D**) ZIF-8, (**E**) ZIF-67, and (**F**) MOF-74 towards RAW 264.7 cells. (ns, no significance; * $p<0.05$, ** $p<0.01$, **** $p<0.0001$).

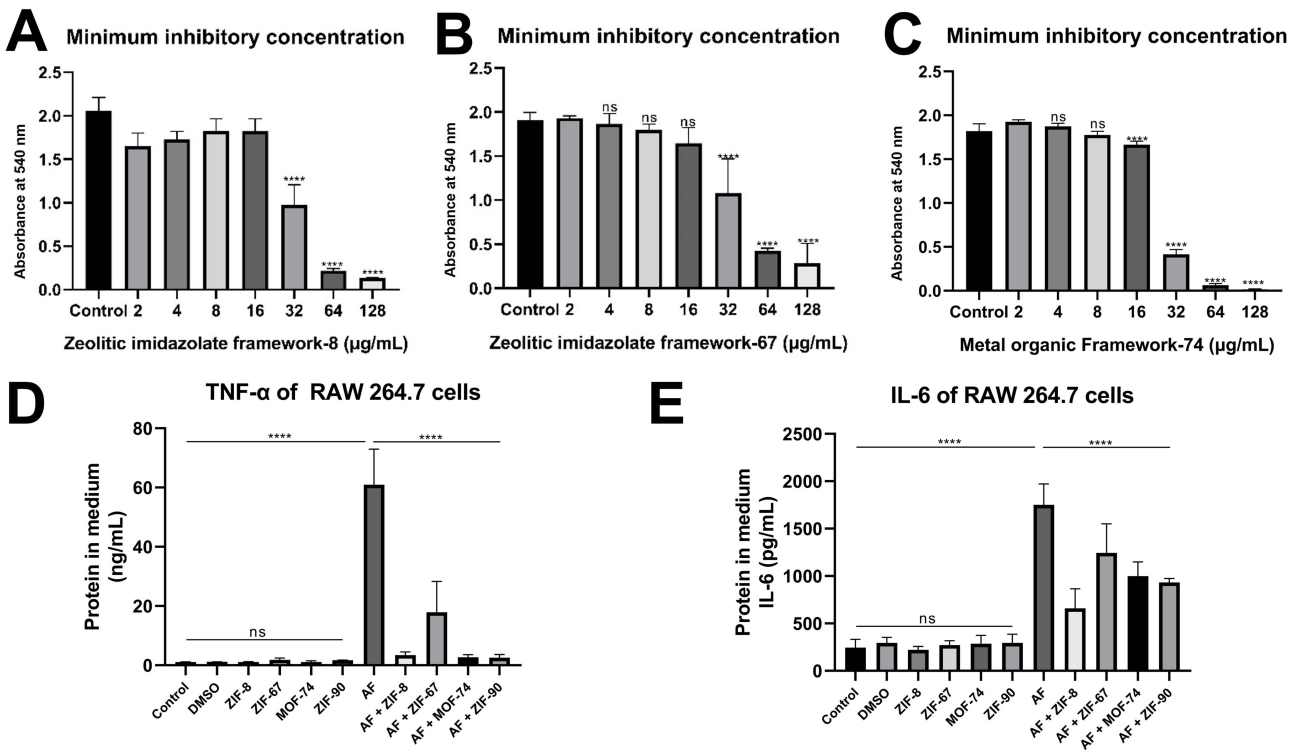

Figure 9 The outcome of antifungal and anti-inflammatory of different MOF materials. Anti- *A. fumigatus* activity of (**A**) ZIF-8, (**B**) ZIF-67, and (**C**) MOF-74 at varying dosages. Effect of ZIF-8, ZIF-67, and MOF-74 on reducing proinflammatory factor content (**D**) TNF-α and (**E**) IL-6 in RAW 264.7 cells. (ns, no significance; **** p<0.0001).

cobalt ions rather than zinc ions. It can be seen that zinc ions in MOF materials have certain anti-fungal effects. And MOF materials containing imidazole groups and MOF-74 (Zn) containing heterocyclic acids have anti-fungal effects. In addition, under the premise of non-toxic to cells, the anti-fungal effect of ZIF-90 is stronger than the other three materials.

Furthermore, we verified the effect of four materials on reducing pro-inflammatory factors in RAW 264.7 cells. We found that all four materials had the effect of reducing pro-inflammatory factors TNF-α and IL-6 at the protein level. Additionally, ZIF-8, MOF-74, and ZIF-90 had better effects on minimizing the pro-inflammatory protein TNF-α than ZIF-67 (Figure 9D and E, $p<0.0001$). The experimental results confirmed that ZIF-8, ZIF-67, MOF-74, and ZIF-90 can lower the pro-inflammatory factors TNF-α and IL-6, so it is beneficial to decrease the inflammatory response.

According to the experimental results, zinc and imidazole ligands in ZIF-90 can jointly exert anti-inflammatory and antifungal effects. This expanded the previous studies on the antibacterial effect of MOF materials containing heterocyclic acid ligands[52] and verified that MOF materials contain imidazole ligands. These outcomes develop the antifungal function of MOF materials.

Conclusion

The effect of ZIF-90 on fungal keratitis was studied in this paper. ZIF-90 can hamper the growth of *A. fumigatus*. ZIF-90 can also prevent excessive immune response and inflammatory response by promoting macrophage apoptosis and reducing mtROS content in macrophages. In addition, ZIF-90 can treat fungal keratitis by reducing corneal scores and inflammatory cell infiltration. Both zinc ions and imidazole ligands of ZIF-90 have anti-inflammatory and antibacterial effects. Moreover, the presence of an aldehyde group on the imidazole ligand enhanced the biocompatibility of ZIF-90. These results suggest that ZIF-90 has good anti-inflammatory properties and immunogenicity, which provides a basis for the treatment of fungal keratitis.

Ethics

Our experiments were conducted in compliance with the Basel Declaration and the ethical standards set by the International Council for Laboratory Animal Science. The study protocol was approved by the Ethics Review Committee of the Affiliated

https://doi.org/10.2147/IJN.S517169

Hospital of Qingdao University, Qingdao, Shandong, China (Approval No. QYFYWZLL29257) in accordance with the ethical principles of the Declaration of Helsinki and informed consent was obtained from all donors.

Acknowledgments

This work was financially supported by the National Natural Science Foundation of China (Nos. 82171029) and the Taishan Scholars Program (Nos. tsqn201812151).

Disclosure

The authors report no conflicts of interest in this work. This paper has been uploaded to arXiv as a preprint: https://doi.org/10.48550/arXiv.2410.20644

References

1. Sharma N, Bagga B, Singhal D, et al. Fungal keratitis: a review of clinical presentations, treatment strategies and outcomes. *Ocul Surf*. 2022;24:22–30. doi:10.1016/j.jtos.2021.12.001
2. Brown L, Leck AK, Gichangi M, Burton MJ, Denning DW. The global incidence and diagnosis of fungal keratitis. *Lancet Infect Dis*. 2021;21(3):e49–e57. doi:10.1016/S1473-3099(20)30448-5
3. Hoffman JJ, Burton MJ, Leck A. Mycotic keratitis-A global threat from the filamentous fungi. *J Fungi*. 2021;7(4). doi:10.3390/jof7040273
4. Gu L, Chi M, Wang Z, et al. Hydroxytyrosol downregulates inflammatory responses via Nrf2/HO-1 axis during fungal keratitis and exerts antifungal effects. *Inter Immunopharmacol*. 2025;149:114202. doi:10.1016/j.intimp.2025.114202
5. Bauer D, Schmitz A, Van Rooijen N, Steuhl KP, Heiligenhaus A. Conjunctival macrophage-mediated influence of the local and systemic immune response after corneal herpes simplex virus-1 infection. *Immunology*. 2002;107(1):118–128. doi:10.1046/j.1365-2567.2002.01477.x
6. Hu J, Hu Y, Chen S, et al. Role of activated macrophages in experimental Fusarium solani keratitis. *Exp Eye Res*. 2014;129:57–65. doi:10.1016/j.exer.2014.10.014
7. Cheng H, Tumpey TM, Staats HF, van Rooijen N, Oakes JE, Lausch RN. Role of macrophages in restricting herpes simplex virus type 1 growth after ocular infection. *Invest Ophthalmol Vis Sci*. 2000;41(6):1402–1409.
8. Nathan C. Nonresolving inflammation redux. *Immunity*. 2022;55(4):592–605. doi:10.1016/j.immuni.2022.03.016
9. Romani L, Puccetti P. Controlling pathogenic inflammation to fungi. *Expert Rev Anti Infect Ther*. 2007;5(6):1007–1017. doi:10.1586/14787210.5.6.1007
10. Mukherjee A, Ghosh KK, Chakrabortty S, Gulyás B, Padmanabhan P, Ball WB. Mitochondrial reactive oxygen species in infection and Immunity. *Biomolecules*. 2024;14(6):670. doi:10.3390/biom14060670
11. Pinegin B, Vorobjeva N, Pashenkov M, Chernyak B. The role of mitochondrial ROS in antibacterial immunity. *J Cell Physiol*. 2018;233(5):3745–3754. doi:10.1002/jcp.26117
12. Jones CG, Stavila V, Conroy MA, et al. Versatile synthesis and fluorescent labeling of ZIF-90 Nanoparticles for biomedical applications. *ACS Appl Mater Interfaces*. 2016;8(12):7623–7630. doi:10.1021/acsami.5b11760
13. Cao P, Cheng Y, Li Z, et al. Intraocular delivery of ZIF-90-RhB-GW2580 nanoparticles prevents the progression of photoreceptor degeneration. *J Nanobiotechnology*. 2023;21(1):44. doi:10.1186/s12951-023-01794-6
14. Lin T, Qin T, Jiang S, Zhang C, Wang L. Anti-inflammatory and anti-biotic drug metronidazole loaded ZIF-90 nanoparticles as a pH responsive drug delivery system for improved pediatric sepsis management. *Microbial Pathogenesis*. 2023;176:105941. doi:10.1016/j.micpath.2022.105941
15. Jiang Z, Wang Y, Sun L, et al. Dual ATP and pH responsive ZIF-90 nanosystem with favorable biocompatibility and facile post-modification improves therapeutic outcomes of triple negative breast cancer in vivo. *Biomaterials*. 2019;197:41–50. doi:10.1016/j.biomaterials.2019.01.001
16. Wang S, Fan Y, Teng J, et al. Nanoreactor based on macroporous single crystals of metal-organic framework. *Small*. 2016;12(41):5702–5709. doi:10.1002/smll.201601873
17. Zhang FM, Dong H, Zhang X, et al. Postsynthetic modification of ZIF-90 for potential targeted Codelivery of two anticancer drugs. *ACS Appl Mater Interfaces*. 2017;9(32):27332–27337. doi:10.1021/acsami.7b08451
18. Chen Y, Cai J, Liu D, et al. Zinc-based metal organic framework with antibacterial and anti-inflammatory properties for promoting wound healing. *Regen Biomater*. 2022;9:rbac019.
19. Wessels I, Maywald M, Rink L. Zinc as a gatekeeper of immune function. *Nutrients*. 2017;9(12). doi:10.3390/nu9121286
20. Jarosz M, Olbert M, Wyszogrodzka G, Młyniec K, Librowski T. Antioxidant and anti-inflammatory effects of zinc. Zinc-dependent NF-κB signaling. *Inflammopharmacology*. 2017;25(1):11–24. doi:10.1007/s10787-017-0309-4
21. Beggs WH, Andrews FA, Sarosi GA. Action of imidazole-containing antifungal drugs. *Life Sci*. 1981;28(2):111–118. doi:10.1016/0024-3205(81)90542-7
22. Perfect JR. The antifungal pipeline: a reality check. *Nat Rev Drug Discov*. 2017;16(9):603–616. doi:10.1038/nrd.2017.46
23. Shieh FK, Wang SC, Leo SY, Wu KC. Water-based synthesis of zeolitic imidazolate framework-90 (ZIF-90) with a controllable particle size. *Chemistry*. 2013;19(34):11139–11142. doi:10.1002/chem.201301560
24. Zhu Y, Peng X, Zhang Y, Lin J, Zhao G. Baicalein protects against aspergillus fumigatus keratitis by reducing fungal load and inhibiting TSLP-induced inflammatory response. *Invest Ophthalmol Vis Sci*. 2021;62(6):26. doi:10.1167/iovs.62.6.26
25. Wilhelmus KR. The Draize eye test. *Surv Ophthalmol*. 2001;45(6):493–515. doi:10.1016/S0039-6257(01)00211-9
26. Montgomery ML, Fuller KK. Experimental models for fungal keratitis: an overview of principles and protocols. *Cells*. 2020;9(7):1713. doi:10.3390/cells9071713
27. Chen H, Geng X, Ning Q, et al. Biophilic positive carbon dot exerts antifungal activity and augments corneal permeation for fungal keratitis. *Nano Lett*. 2024;24(13):4044–4053. doi:10.1021/acs.nanolett.4c01042

28. Yuan H, Wu Y, Pan X, Gao L, Xiao G. Pyridyl ionic liquid functionalized ZIF-90 for catalytic conversion of CO2 into cyclic carbonates. *Catalysis Letters*. 2020;150(12):3561–3571. doi:10.1007/s10562-020-03259-z
29. Suman S, Kumar A, Saxena I, Kumar M. Fungal keratitis: recent advances in diagnosis and treatment. *Infect Eye Dis Recent Adv Diagn Treat*. 2021;55(10.5772).
30. Reginatto P, Agostinetto GJ, Fuentefria RDN, Marinho DR, Pizzol MD, Fuentefria AM. Eye fungal infections: a mini review. *Arch Microbiol*. 2023;205(6):236. doi:10.1007/s00203-023-03536-6
31. Ramage G, Ghannoum MA, López-Ribot JL. Fungal biofilms: agents of disease and drug resistance. *Molecular Principles of Fungal Pathogenesis*. 2006;177–185.
32. Makabenta JMV, Nabawy A, Li CH, Schmidt-Malan S, Patel R, Rotello VM. Nanomaterial-based therapeutics for antibiotic-resistant bacterial infections. *Nat Rev Microbiol*. 2021;19(1):23–36. doi:10.1038/s41579-020-0420-1
33. Liu S, Le Mauff F, Sheppard DC, Zhang S. Filamentous fungal biofilms: conserved and unique aspects of extracellular matrix composition, mechanisms of drug resistance and regulatory networks in Aspergillus fumigatus. *NPJ Biofilms Microbiomes*. 2022;8(1):83. doi:10.1038/s41522-022-00347-3
34. Hsueh YH, Ke WJ, Hsieh CT, Lin KS, Tzou DY, Chiang CL. ZnO nanoparticles affect Bacillus subtilis cell growth and biofilm formation. *PLoS One*. 2015;10(6):e0128457. doi:10.1371/journal.pone.0128457
35. Wu L, Fan L, Shi L, et al. Synthesis, characterization and antifungal activity of imidazole chitosan derivatives. *Carbohydr Res*. 2024;544:109238. doi:10.1016/j.carres.2024.109238
36. Lee Y, Puumala E, Robbins N, Cowen LE. Antifungal drug resistance: molecular mechanisms in candida albicans and beyond. *Chem Rev*. 2021;121(6):3390–3411. doi:10.1021/acs.chemrev.0c00199
37. Rodríguez-Morales P, Franklin RA. Macrophage phenotypes and functions: resolving inflammation and restoring homeostasis. *Trends Immunol*. 2023;44(12):986–998. doi:10.1016/j.it.2023.10.004
38. Medina CB, Mehrotra P, Arandjelovic S, et al. Metabolites released from apoptotic cells act as tissue messengers. *Nature*. 2020;580(7801):130–135. doi:10.1038/s41586-020-2121-3
39. Mittal M, Siddiqui MR, Tran K, Reddy SP, Malik AB. Reactive oxygen species in inflammation and tissue injury. *Antioxidants & Redox Signaling*. 2014;20(7):1126–1167. doi:10.1089/ars.2012.5149
40. Feng Y, Wu Y, Duan R, Wang P, Zhong X, Wu X. Structural characterization and anti-inflammatory effects of enteromorpha prolifera polysaccharide-Fe/Zn complexes. *Int J Biol Macromol*. 2023;253(Pt 6):127166. doi:10.1016/j.ijbiomac.2023.127166
41. Raza W, Yang X, Wu H, Huang Q, Xu Y, Shen Q. Evaluation of metal ions (Zn(2+), Fe(3+) and Mg(2+)) effect on the production of fusaricidin-type antifungal compounds by Paenibacillus polymyxa SQR-21. *Bioresour Technol*. 2010;101(23):9264–9271. doi:10.1016/j.biortech.2010.07.052
42. Jiao L, Lin F, Cao S, et al. Preparation, characterization, antimicrobial and cytotoxicity studies of copper/zinc- loaded montmorillonite. *J Anim Sci Biotechnol*. 2017;8(1):27. doi:10.1186/s40104-017-0156-6
43. Gu L, Lin J, Wang Q, et al. Mesoporous zinc oxide-based drug delivery system offers an antifungal and immunoregulatory strategy for treating keratitis. *J Controlled Release*. 2024;368:483–497. doi:10.1016/j.jconrel.2024.03.006
44. Abbondante S, Leal SM, Clark HL, et al. Immunity to pathogenic fungi in the eye. *Semin Immunol*. 2023;67:101753. doi:10.1016/j.smim.2023.101753
45. Gupta AK, Nicol K, Batra R. Role of antifungal agents in the treatment of seborrheic dermatitis. *Ame J Clin Dermatol*. 2004;5(6):417–422. doi:10.2165/00128071-200405060-00006
46. Muheyuddeen G, Khan MY, Ahmad T, et al. Design, synthesis, and biological evaluation of novel imidazole derivatives as analgesic and anti-inflammatory agents: experimental and molecular docking insights. *Scientific Reports*. 2024;14(1):23121. doi:10.1038/s41598-024-72399-8
47. Ramos D, Aguila-Rosas J, Quirino-Barreda CT, et al. Linezolid@MOF-74 as a host-guest system with antimicrobial activity. *J Mater Chem B*. 2022;10(48):9984–9991. doi:10.1039/D2TB01819E
48. Hsu PH, Chang CC, Wang TH, et al. Rapid fabrication of biocomposites by encapsulating enzymes into Zn-MOF-74 via a mild water-based approach. *ACS Appl Mater Interfaces*. 2021;13(44):52014–52022. doi:10.1021/acsami.1c09052
49. El Ouardi M, El Aouni A, Ait Ahsaine H, Zbair M, BaQais A, Saadi M. ZIF-8 metal organic framework composites as hydrogen evolution reaction photocatalyst: a review of the current state. *Chemosphere*. 2022;308(Pt 3):136483. doi:10.1016/j.chemosphere.2022.136483
50. Wang Y, Zeng M, Fan T, et al. Biomimetic ZIF-8 nanoparticles: a novel approach for biomimetic drug delivery systems. *Int J Nanomedicine*. 2024;19:5523–5544. doi:10.2147/IJN.S462480
51. Zeng Y, Liao D, Kong X, et al. Current status and prospect of ZIF-based materials for breast cancer treatment. *Colloids Surf B Biointerfaces*. 2023;232:113612. doi:10.1016/j.colsurfb.2023.113612
52. Li R, Chen T, Pan X. Metal–organic-framework-based materials for antimicrobial applications. *ACS Nano*. 2021;15(3):3808–3848. doi:10.1021/acsnano.0c09617